Apparent "three-dimensional" Fermi surface of transition-metal monolayers

O. Rader, H. Wolf,* and W. Gudat
Helmholtz-Zentrum Berlin für Materialien und Energie, Elektronenspeicherring BESSY II, Albert-Einstein-Straße 15, D-12489 Berlin, Germany

A. Tadich,† L. Broekman, E. Huwald, R. C. G. Leckey, and J. D. Riley
Department of Physics, La Trobe University, Bundoora, Victoria 3083, Australia

A. M. Shikin
Institute of Physics, St. Petersburg State University, St. Petersburg 198904, Russia

F. Matsui, H. Miyata,‡ and H. Daimon
Graduate School of Materials Science, Nara Institute of Science and Technology, Nara 630-0192, Japan
(Received 10 March 2009; published 2 June 2009)

One of the fundamental properties of an electronic system is its dimensionality. Novel photoemission apparatuses enable a direct determination of the Fermi surface of metals in all three dimensions but the data obtained from transition-metal monolayers appears to defy established experimental and theoretical insights. Our experimental approach resolves all of the existing conflicts surrounding Ni/Cu(100) and similar systems. We suggest the measurement of Fermi-surface projections to optimize spin-dependent transport properties.

DOI: 10.1103/PhysRevB.79.245104 PACS number(s): 71.18.+y, 73.20.Hb, 79.60.Bm, 79.60.Jv

I. INTRODUCTION

The world that surrounds us is made of three-dimensional objects and this fact determines their physical properties. On the lengthscale of the atomic interactions, however, one distinguishes between three-, two-, and lower dimensionality. The quantum Hall effect, the layered high-T_C superconductors, and the oscillatory magnetic interlayer coupling of giant magnetoresistive (GMR) multilayers all reveal important aspects of two-dimensional physics in three-dimensional matter. Experimental progress has in recent years enabled the measurement of Fermi surfaces in three dimensions by photoelectron spectroscopy so that several studies exist by now with bulk Cu chosen as a prototype system.[1,2] Motivated by the GMR applications of Co/Cu and Ni/Cu multilayers,[3] photoelectron spectroscopy has recently been applied to ultrathin Ni and Co films to obtain the Fermi-surface geometry in momentum space directions parallel and perpendicular to the film plane. In the photoemission experiment it was found that 1 monoatomic layer (ML) Ni/Cu(100) displays a Fermi surface which is identical to that of bulk Ni, as represented by a 6 ML film.[4] More precisely, the angle distribution pattern of electrons from the Fermi level was found to vary between photon energies $h\nu$=45 and 90 eV in exactly the same way for 1 and 6 ML and clearly differently from that of Cu(100). Furthermore, the width of the Ni *d* band does not change between the monolayer and bulk Ni. These findings for Ni and also for Co were interpreted as resulting from a three-dimensional electronic structure in the monolayer attributed to the short screening length of electrons in metals, the similarity of Ni and Cu cores, charge transfer which acts to smoothen out the 2 eV potential step between Ni and Cu, and Ni-Cu hybridization.[4]

On the other hand, inverse photoemission of 1–5 ML Ni/Cu(100) reveals distinct quantum-well states above the Fermi energy (E_F) proving strong electron confinement in the Ni layer.[5] Angle-resolved photoemission along [100] showed at constant photon energy that the Ni *d* band changes with thickness and is narrower for 1 ML Ni/Cu(100) than for bulk Ni, a result which agrees with the theoretical expectation for systems of reduced dimensionality.[6] This is important for the magnetism of Ni since band narrowing in this strong ferromagnet leads to a reduced magnetic moment which is indeed experimentally observed at the Ni/Cu interface.[7] There are, therefore, important unresolved problems in terms of the findings in Ref. 4. Moreover, the same authors conclude in a subsequent study of thick Co/Cu(100),[8] that for 21–45 eV photon energy, the angle distribution does not correspond to the shape of the Fermi surface but to the structure of the final states. This was explained by the flatness of the $E(\mathbf{k})$ dispersion of transition-metal *d* bands.[8] Because final states are three dimensional, this result raises the question whether the three dimensionality of the Ni and Co monolayers[4] is a final-state effect as well. Other theoretical studies also note the role of the final state in Fermi-surface measurements, and first calculations have been published for bulk Ni.[9]

The present situation is unsatisfactory leaving fundamental questions open: (i) Are the experimental findings[4] reproducible? (ii) Are the expectations for the electronic structure from reduced dimensionality wrong when the Fermi surface is considered or when Ni/Cu(100) is concerned? (iii) The magnetic interlayer coupling is described based on electron confinement in multilayers.[10] How can the GMR effect exist despite formation of a three-dimensional electronic structure and Fermi surface at Ni/Cu and Co/Cu interfaces? (iv) How can the contradiction with quantum-well states be resolved? (v) What does the alleged three-dimensionality mean for itinerant magnetism in low dimensions? (vi) Can we learn anything about the Fermi surface of transition metals from photoemission and can we discuss its dimensionality despite final-state effects? (vii) If confinement is really so weak, is

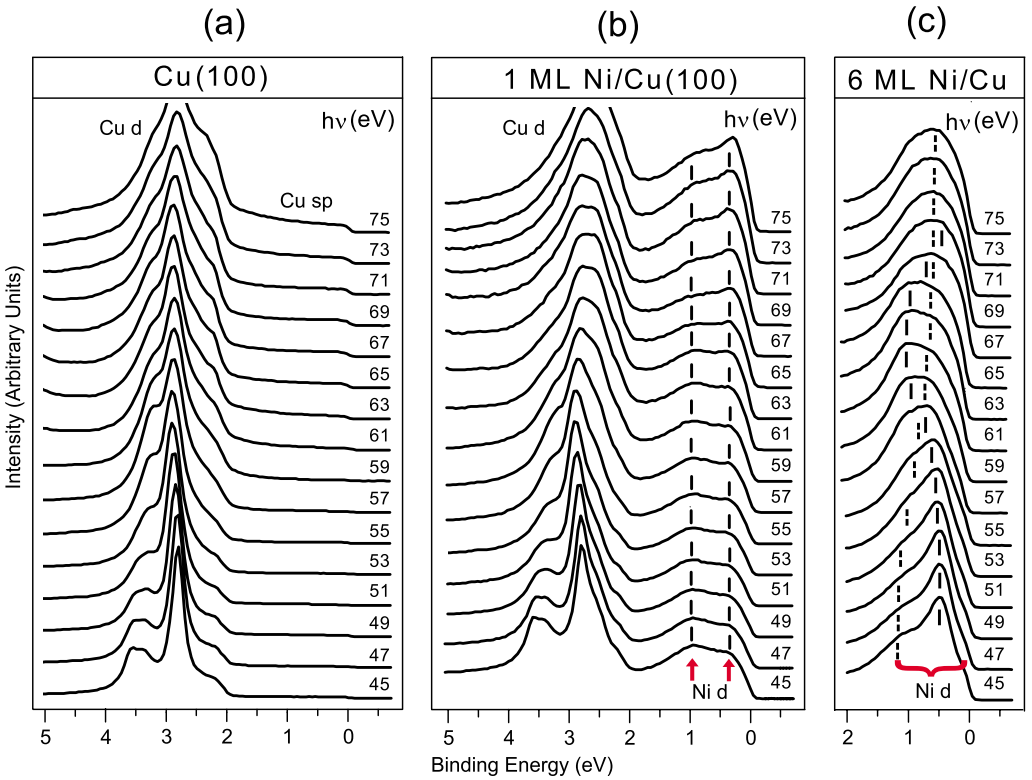

FIG. 1. (Color online) Angle-resolved photoemission in normal emission. Ni *d* states do not disperse with $h\nu$ or $\mathbf{k}_\perp$ for 1 ML (two-dimensional) but disperse strongly for 6 ML Ni (three-dimensional). For 1 ML, ticks mark $\bar{\Gamma}_1$ states at 0.9 eV and $\bar{\Gamma}_5$ states at 0.3 eV. For 6 ML, solid ticks mark Δ_1 states and dashed ticks mark Δ_5 states.

much stronger confinement possible by cutting off remaining interactions, and which novel transport and spin-transport effects might result?

II. EXPERIMENTAL

Photoemission experiments have been conducted with linearly polarized light with a display-type analyzer,[2] a hemispherical analyzer (Fig. 1), and a second generation toroidal analyzer[11] (Figs. 2–5). Samples were prepared as described previously[6] and measured at room temperature. All measurements are for the (100)-surface, therefore, we will refer to the systems simply as Cu, 1 ML Ni, and 6 ML Ni.

III. NORMAL-EMISSION PHOTOELECTRON SPECTRA

Normal emission spectra are shown in Fig. 1 for clean Cu, 1 ML Ni, and 6 ML Ni. Conventionally, the photon energy is varied to probe direct transitions into free-electron final states which corresponds to varying the electron wave vector perpendicular to the surface normal ($\mathbf{k}_\perp$) along ΓX. It is seen that the *d* states in Cu around 2–4 eV binding energy show a significant dispersion with $\mathbf{k}_\perp$, especially after surface photoemission is removed by Ni deposition [Fig. 1(b)], and about the same dispersion occurs with the *d* states of 6 ML Ni which are situated 2 eV higher, at E_F. In contrast, the Ni *d* states of 1 ML Ni (red arrows) stay at fixed binding energy without any dispersion. This textbook example of reduced dimensionality of the electronic structure of a monolayer film is in stark contrast to the formation of a three-dimensional Ni electronic structure found in Ref. 4.

IV. ANGLE DISTRIBUTION AT E_F

Figure 2 shows for $h\nu$=60 eV the angular distribution of photoelectrons from E_F plotted *vs.* $\mathbf{k}_\parallel=(k_x,k_y)$, i.e., the electron wave vector components parallel to the surface plane. The measurement was achieved by azimuthal scans. During an azimuthal scan the sample rotates about its surface normal while electrons emitted along polar angles −90° to +90° are measured simultaneously.[11,12] In Figs. 2(a)–2(d) we see the distribution from clean Cu with features from the belly of the Fermi surface in the first and second Brillouin zone. Dominating features in the first Brillouin zone are in Fig. 2(a) intense and broad emissions (A) situated inside of a circle at 1.1 Å^{-1}. Intense features in Fig. 2(d) define again a circle (B) but it is larger (1.3 Å^{-1}) than in Fig. 2(a) even though only the light polarization has changed. The sharp emission B occurs along [0$\bar{1}$1]. Along this direction, the Cu Fermi surface has necks which lead to small bulk band gaps at E_F when projected onto (100). Feature B was recently observed and attributed to a surface state[13] which is well known from photoemission at the $\bar{X}$-point of Cu(100).[14]

Figures 2(b) and 2(c) show that feature A is preserved at 1 ML Ni (here partially due to Cu background) and becomes

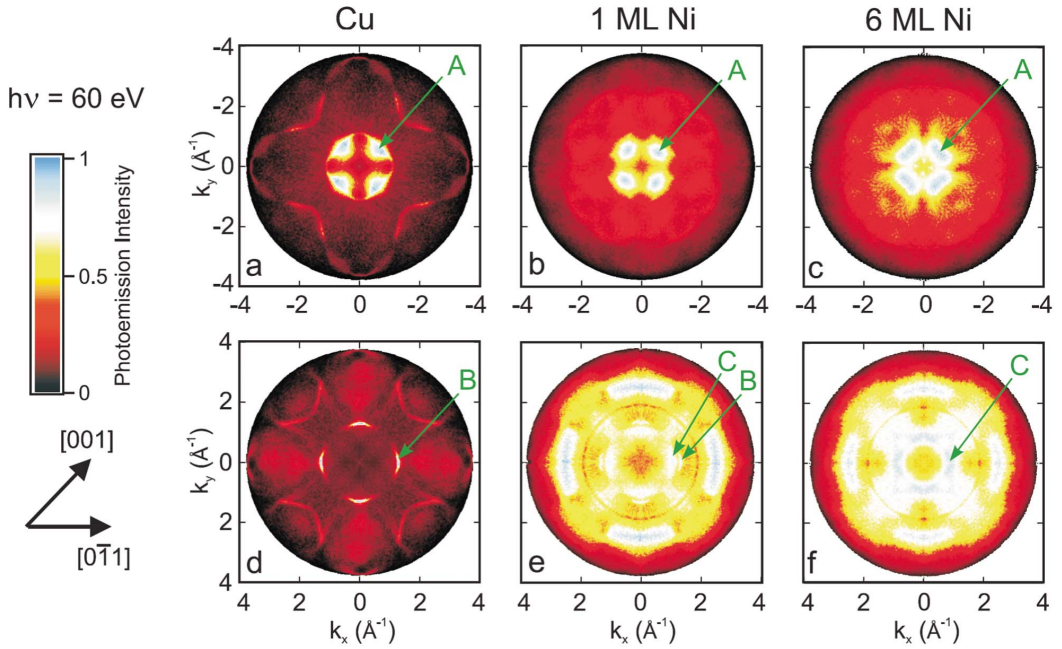

FIG. 2. (Color online) Angle distribution of photoemission intensity at E_F, $h\nu$=60 eV. Predominantly $\mathbf{k} \perp \mathbf{E}$ (top) and $\mathbf{k} \| \mathbf{E}$ (bottom) (Ref. 12). Fermi-surface contours are similar for 1 and 6 ML Ni and very different from those of Cu.

slightly more elongated for 6 ML. Considering feature B, some intensity is left for 1 ML [Fig. 2(e)]. This persistence, unexpected for a surface state, comes along with the appearance of a similar feature C with slightly smaller $k_\|$ (1.05 Å^{-1}) which dominates the pattern together with other new features. [The red circle at $k_\| \approx 2$ Å^{-1} in Fig. 2(e) is an artefact of the detector.] Feature C appears very similarly for 6 ML (f) but somewhat closer to the center ($k_\|$=0.9 Å^{-1}). Also Figs. 2(b) and 2(c) show A-type features similar to each other. Thus for both light-incidence geometries, the overall appearance of 1 ML and 6 ML Ni is, in spite of some differences, rather similar confirming for $h\nu$=60 eV the previous finding of a certain thickness independence.[4]

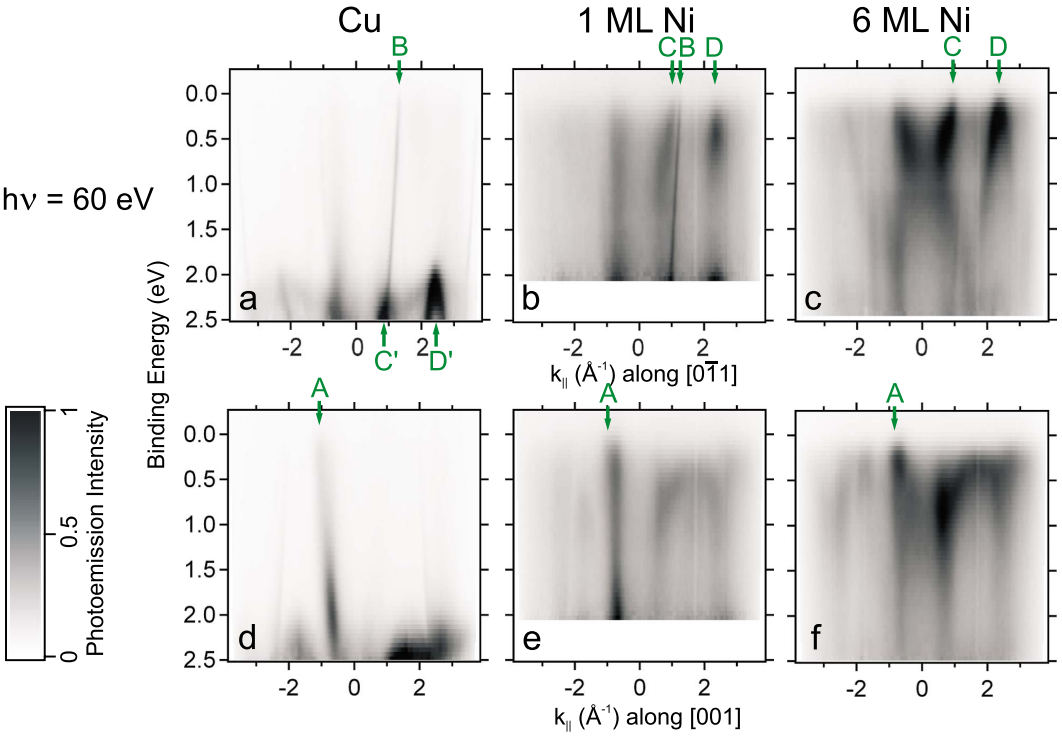

FIG. 3. (Color online) Angle-dependent photoemission spectra, $h\nu$=60 eV (Ref. 12). Dispersions with $\mathbf{k}_\|$ are less pronounced for 1 ML than for 6 ML Ni while they intersect E_F at similar $\mathbf{k}_\|$ vectors.

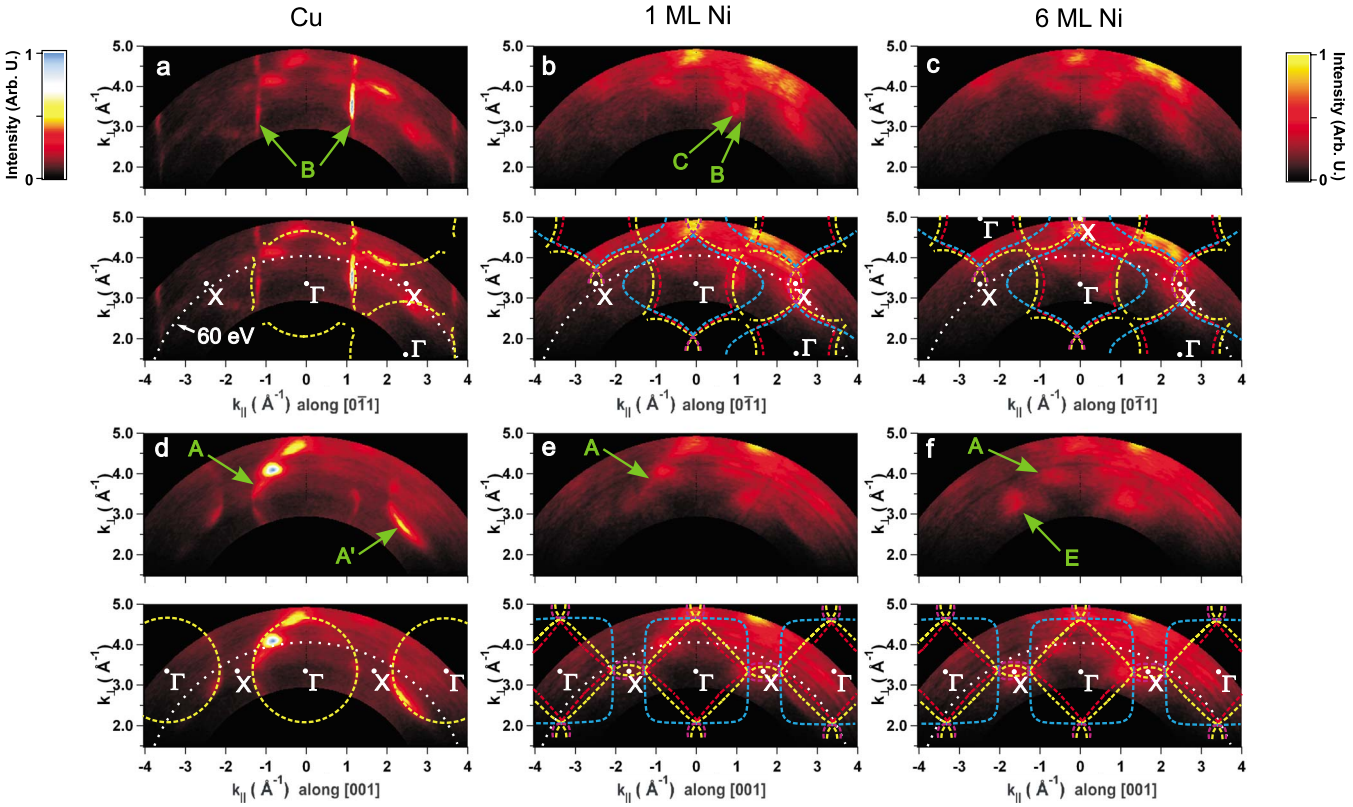

FIG. 4. (Color online) Angle-resolved constant-initial-state spectroscopy at E_F. Characteristic features C of 1 ML Ni and E of bulk Ni appear in Cu band gaps which prevent coupling to the substrate.

V. ANGLE-DEPENDENT PHOTOELECTRON SPECTRA

Angle-dependent photoemission spectra were taken through both [0$\bar{1}$1] and [001] azimuths as shown in Fig. 3.[12] For Cu, we can identify the features which cross E_F, i. e., A and B, both of which disperse with $k_\parallel$, and other d-type features around 2 eV binding energy (C′, D′). Concerning feature B, its dispersion from E_F downward by 2 eV connecting it to the d states shows that it is a three-dimensional feature and not the two-dimensional surface state claimed before[13] because that surface state disperses very differently forming a parabola which reaches its bottom already 58 meV below E_F.[14]

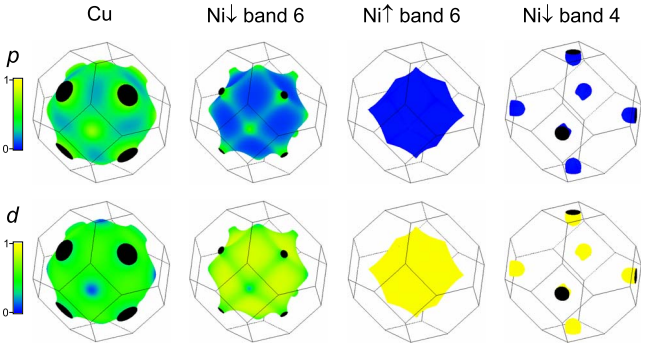

FIG. 5. (Color online) Calculated orbital character at E_F of Cu and Ni bands compiled using Ref. 17. The fourth minority-spin band of Ni (Ni↓ band 4) corresponds to feature E in Fig. 4(f) which develops for 6 ML Ni and not for 1 ML Ni. It is of pure d character.

Turning to Ni and comparing monolayer and bulk dispersions of features C and D shows that these bands cross E_F at similar $\mathbf{k}_\parallel$ vectors for 1 and 6 ML Ni but each disperses in very different ways with $\mathbf{k}_\parallel$ for 1 and 6 ML Ni. For thick Ni each band shows a much more pronounced $\mathbf{k}_\parallel$ dependence, in particular along [0$\bar{1}$1]. Even though the Fermi surface has a similar appearance, the Ni monolayer can clearly be distinguished from bulklike Ni when comparing the band dispersion away from E_F not only with $\mathbf{k}_\perp$ as in Fig. 1 but already with $\mathbf{k}_\parallel$. This observation reconciles conclusions drawn from Figs. 1 and 2.

Concerning the Ni features A, C, and D, we note that their intensity is highest near E_F and rapidly drops at higher binding energy. This was recently measured for Ni(100) (Ref. 15) and studied in detail employing one-step photoemission calculations.[9] The intensity drop was explained in terms of a final-state gap at 43 eV. In the calculation,[9] the effect depends sensitively on the photon energy and requires $42\ \text{eV} < h\nu < 43.5\ \text{eV}$. This explanation may, however, not be appropriate in view of the photon energy of 60 eV used in Fig. 3, and this calls the suitability of the theoretical description into question.

VI. ANGLE-RESOLVED CONSTANT-INITIAL STATE SPECTROSCOPY (ARCIS)

A central observation in Ref. 4 is the photon energy dependence of monolayers. We show in Fig. 4 ARCIS spectra at E_F by scanning the photon energy from 30 eV (inner arc)

to 90 eV (outer arc). The spectra have been mapped absolutely in $\mathbf{k}$ by employing a free-electron final state with an inner potential of 12 eV. The Cu feature B appears without dependence on $\mathbf{k}_\perp$. The broader feature A follows the predominantly spherical shape of the Cu Fermi surface with $\mathbf{k}_\perp$ and can also be observed very clearly as A′ in the neighboring Brillouin zone and at lower photon energies, also <45 eV. Looking at Figs. 4(b) and 4(c) and Figs. 4(e) and 4(f), the first impression is that of a very similar $\mathbf{k}_\parallel$ dependence of 1 and 6 ML Ni as was reported before.[4] The Ni features appear less defined than the Cu features. Moreover, most features observed for Ni in Figs. 4(b), 4(c), 4(e), and 4(f) already appear with similar intensity modulation for Cu. The modulation, e.g., the strong intensity at $\mathbf{k}_\perp = 4.2$ Å^{-1}, is not due to initial states, in Figs. 4(a) and 4(d). These are final-state effects in Cu and Ni, and they are not caused by the flatness of d bands[8] because the states at the Fermi surface of Cu are neither d nor flat.

Reference 4 suggests as reason the short electron screening length and charge transfer smearing out a 2 eV potential step between Ni and Cu. There is, however, no need to invoke such arguments because practically no interface charge transfer occurs already in the single-particle picture of local-density theory without any screening [~0.01 electrons/atom from Ni to Cu (Ref. 16)]. It is hence not straightforward to attribute any special qualities to the Fermi energy except that for Cu, band gaps at E_F are small. We have seen strong two-dimensional confinement for energies below E_F in Fig. 1. Considering E_F directly, we can in the entire Fig. 4 see only two Ni features that do not appear similarly in Cu: One is the sharp feature C for 1 ML Ni. The other one is the feature E at the X point in 6 ML Ni. C is a monolayer sp feature which for 6 ML Ni moves away and broadens in $\mathbf{k}$, and E is from the bulk majority spin Fermi surface (pure d-character according to Ref. 17) which is invisible in the Ni monolayer data because the bulk Ni Fermi surface has not yet developed as a whole. Figure 4 shows that C and E have in common that they are the only features which are situated in the rare gaps of the Fermi surface of the Cu substrate projected on (100): C inside of the necks at the L-point and E at X in between the spheres. These gaps are crucial in confining Ni electrons at E_F to the overlayer the thickness of which determines the dimensionality.

VII. CONCLUSION

The questions posed at the outset can now be answered: (i) The experimental behavior is confirmed. (ii) Simple expectations from the ground-state electronic structure about dimensionality and confinement are fulfilled. There is no need to invoke a particular role of the electrons at E_F. For the Fermi surface, the (100)-projection of the bulk Ni states on the bulk Cu states is to be considered. Only regions which jut out are two-dimensionally confined, the large degenerate regions are potentially three-dimensionally extended, however, quantum-well resonances are possible and do occur. (iii) In particular, the caliper vectors[10] describing long-range oscillatory magnetic coupling in GMR systems are an example of such resonances. (iv) Consider intensities. The quantum-well states and resonances are present along with three-dimensional bulk direct transitions which in the spectra are often spectroscopically suppressed by choosing, e.g., for Cu(100)-derived quantum wells either $h\nu > 15$ eV (Ref. 10) or $h\nu < 10$ eV.[18] While in previous normal-emission measurements[10,18] the bulk transitions did not compete for spectral weight, they dominate the present Fermi-surface scans. (v) Consider symmetries. Figure 1(b) shows two Ni peaks but these have contributions from two pairs of exchange-split states of even and odd symmetry.[6] The even-symmetry ones have the character of resonances whereas the odd-symmetry ones are fully confined. The confinement is indeed strong because apparently bulk direct transitions in Ni are not spectroscopically suppressed and would appear under the measurement conditions in Fig. 1 if they were strong. Nevertheless, normal-emission Ni features are weak as compared to off-normal ones as seen directly in Figs. 3(b) and 3(e). Unlike previously suggested,[4] the Ni d states cannot hybridize with substrate Cu d states due to the large energy separation (~2 eV). The Ni $3d$ magnetic moment is reduced at the interface due to confinement-induced band narrowing and sp-d hybridization within Ni. The symmetry-allowed Ni d states can hybridize with Cu sp states but the spacial localization of the Ni $3d$ wave functions (about 1/2 of the nearest-neighbor distance) prevents extension of an induced moment into Cu. Even at the Co/Cu interface with ~3× larger magnetic moment, the Cu moment is only $0.05\mu_B$.[19] (vi) There is much progress in calculating final-state effects[8,9] but the comparison to experiment is not convincing as yet. Final-state effects are strong but they do not obscure our insight into dimensionality. (vii) Much stronger confinement is indeed possible but it will be interesting whether it can be achieved to tune spin-transport properties as they will depend on the ratio between majority- and minority-spin transmissions. It has been argued that reliable calculations of spin-dependent transport must in the future use Fermi-surface projections as employed here.[20] This emphasizes the potential of Fermi-surface measurements by angle-resolved photoemission for magnetotransport, in particular when spin resolution is added.

Note added. The reader is suggested to consider also Ref. 21 which was published after the submission of the present paper.

ACKNOWLEDGMENTS

O.R. acknowledges fruitful discussions with C. Carbone, kind hospitality by H. Namba and his group at Ritsumeikan Synchrotron Radiation Center, and Alexander von Humboldt foundation for a travel grant. The Australian component is funded by the Australian Research Council.

*Present address: Department Temperature, Physikalisch-Technische Bundesanstalt, Abbestraße 2-12, D-10587 Berlin, Germany.

†Present address: Australian Synchrotron, 800 Blackburn Road, Clayton 3168, Victoria, Australia.

‡Present address: Toray Research Center, Otsu, Shiga 520-8567, Japan.

[1] J. A. Con Foo, A. P. J. Stampfl, A. Ziegler, B. Mattern, M. Hollering, R. Denecke, L. Ley, J. D. Riley, and R. C. G. Leckey, Phys. Rev. B **53**, 9649 (1996); M. Hochstrasser, N. Gilman, R. F. Willis, F. O. Schumann, J. G. Tobin, and E. Rotenberg, *ibid.* **60**, 17030 (1999); T. Dütemeyer, C. Quitmann, M. Kits, K. Dörnemann, L. S. O. Johansson, and B. Reihl, Rev. Sci. Instrum. **72**, 2638 (2001); M. Kotsugi, W. Kuch, F. Offi, L. I. Chelaru, and K. Kirschner, *ibid.* **74**, 2754 (2003); M. Bovet, V. N. Strocov, F. Clerc, C. Koitzsch, D. Naumovic, and P. Aebi, Phys. Rev. Lett. **93**, 107601 (2004).

[2] F. Matsui, H. Miyata, O. Rader, Y. Hamada, Y. Nakamura, K. Nakanishi, K. Ogawa, H. Namba, and H. Daimon, Phys. Rev. B **72**, 195417 (2005).

[3] M. T. Johnson, S. T. Purcell, N. W. E. McGee, R. Coehoorn, J. aan de Stegge, and W. Hoving, Phys. Rev. Lett. **68**, 2688 (1992); W. Schwarzacher and D. S. Lashmore, IEEE Trans. Magn. **32**, 3133 (1996).

[4] G. J. Mankey, K. Subramanian, R. L. Stockbauer, and R. L. Kurtz, Phys. Rev. Lett. **78**, 1146 (1997).

[5] F. J. Himpsel and O. Rader, Appl. Phys. Lett. **67**, 1151 (1995).

[6] C. Pampuch, O. Rader, R. Kläsges, and C. Carbone, Phys. Rev. B **63**, 153409 (2001).

[7] P. Srivastava, N. Haack, H. Wende, R. Chauvistré, and K. Baberschke, Phys. Rev. B **56**, R4398 (1997).

[8] X. Gao, A. N. Koveshnikov, R. H. Madjoe, R. L. Stockbauer, and R. L. Kurtz, Phys. Rev. Lett. **90**, 037603 (2003).

[9] S. Sahrakorpi, M. Lindroos, and A. Bansil, Phys. Rev. B **66**, 235107 (2002).

[10] J. E. Ortega, F. J. Himpsel, G. J. Mankey, and R. F. Willis, Phys. Rev. B **47**, 1540 (1993).

[11] L. Broekman, A. Tadich, E. Huwald, J. Riley, R. Leckey, T. Seyller, K. Emtsev, and L. Ley, J. Electron Spectrosc. Relat. Phenom. **144-147**, 1001 (2005).

[12] With *p*-polarized light at 45° off-normal incidence this distinguishes two conditions: electron emission toward the light-incidence direction (predominantly $\mathbf{k} \perp \mathbf{E}$; we define $k_{\parallel} < 0$ for this geometry) and away from light incidence (predominantly $\mathbf{k} \parallel \mathbf{E}$; $k_{\parallel} > 0$).

[13] J. Martínez-Blanco, V. Joco, J. Fujii, P. Segovia, and E. G. Michel, Phys. Rev. B **77**, 195418 (2008).

[14] S. D. Kevan, Phys. Rev. B **28**, 2268 (1983).

[15] K. N. Altmann, D. Y. Petrovykh, G. J. Mankey, N. Shannon, N. Gilman, M. Hochstrasser, R. F. Willis, and F. J. Himpsel, Phys. Rev. B **61**, 15661 (2000).

[16] S. K. Ghosh, H. G. Salunke, G. P. Das, A. K. Grover, and M. K. Totlani, Bull. Mater. Sci. **22**, 761 (1999).

[17] C. Lehmann, S. Sinning, P. Zahn, H. Wonn, and I. Mertig, http://www.physik.tu-dresden.de/~fermisur/.

[18] C. Carbone, E. Vescovo, R. Kläsges, D. D. Sarma, and W. Eberhardt, J. Magn. Magn. Mater. **156**, 259 (1996).

[19] M. G. Samant, J. Stöhr, S. S. P. Parkin, G. A. Held, B. D. Hermsmeier, F. Herman, M. van Schilfgaarde, L.-C. Duda, D. C. Mancini, N. Wassdahl, and R. Nakajima, Phys. Rev. Lett. **72**, 1112 (1994).

[20] A. Brataas, G. E. W. Bauer, and P. J. Kelly, Phys. Rep. **427**, 157 (2006).

[21] M. Hoesch, V. N. Petrov, M. Muntwiler, M. Hengsberger, J. L. Checa, T. Greber, and J. Osterwalder, Phys. Rev. B **79**, 155404 (2009).